DMD Fast Forward. Published on June 15, 2015 as DOI: 10.1124/dmd.115.065326
This article has not been copyedited and formatted. The final version may differ from this version.

Determination of a degradation constant for CYP3A4 by direct suppression of mRNA in a novel human hepatocyte model, HepatoPac™

Diane Ramsden, Jin Zhou and Donald J. Tweedie

Drug Metabolism and Pharmacokinetics, Boehringer Ingelheim Pharmaceuticals, Inc., Ridgefield, Connecticut, USA (D.R., J.Z., D.J.T)

DMD Fast Forward. Published on June 15, 2015 as DOI: 10.1124/dmd.115.065326
This article has not been copyedited and formatted. The final version may differ from this version.

RUNNING TITLE: Derivation of CYP3A4 k_{deg} in Human HepatoPac

Please address correspondence to:

Diane Ramsden

Drug Metabolism & Pharmacokinetics

Research and Development

Boehringer Ingelheim Pharmaceuticals, Inc.,

900 Ridgebury Rd., Ridgefield, CT 06877, USA.

Phone: (203) 798-5793

Fax: (203) 791-6003

E-mail: diane.ramsden@boehringer-ingelheim.com.

Number of

Text pages: 17

Tables: 5

Figures: 5

References: 55

Number of Words

Abstract: 245

Introduction: 747

Discussion: 1,484

Non standard Abbreviations**:**

AIC: Akaike information criterion, P450: cytochromes P450; DDI, drug drug interaction; DMEs, drug metabolizing enzymes; hHCM: Human HepatoPac culture medium; hHPM : Human HepatoPac probing medium; HLM, human liver microsomes; IL6, interleukin 6 ; LC-MS/MS, high performance liquid chromatography-tandem mass spectrometry; siRNA, small interfering RNA

DMD Fast Forward. Published on June 15, 2015 as DOI: 10.1124/dmd.115.065326
This article has not been copyedited and formatted. The final version may differ from this version.

Abstract

Accurate determination of rates of *de novo* synthesis and degradation of cytochromes P450 (P450) has been challenging. There is a high degree of variability in the multiple published values of turnover for specific P450s which is likely exacerbated by differences in methodologies. For CYP3A4, half-life values range from 10 to 140h (Yang et al., 2008). An accurate value for k_{deg} has been identified as a major limitation for prediction of drug interactions involving mechanism based inhibition and/or induction. Estimation of P450 half-life from *in vitro* test systems, such as human hepatocytes, is complicated by differential decreased enzyme function over culture time, attenuation of the impact of enzyme loss through inclusion of glucocorticoids in media, and viability limitations over long-term culture times. HepatoPac overcomes some of these challenges providing an extended stability of enzymes (2.5 weeks in our hands). As such it is a unique tool for studying rates of enzyme degradation achieved through modulation of enzyme levels. CYP3A4 mRNA levels were rapidly depleted by >90% using either siRNA or addition of IL6 which allowed an estimation of the degradation rate constant for CYP3A protein over an incubation time of 96 hours. The degradation rate constant of $0.0240 \pm 0.005\ h^{-1}$ was reproducible in hepatocytes from five different human donors. These donors also reflected the overall population with respect to CYP3A5 genotype. This methodology can be applied to additional enzymes and may provide a more accurate *in vitro* derived k_{deg} value for predicting clinical DDI outcomes.

DMD Fast Forward. Published on June 15, 2015 as DOI: 10.1124/dmd.115.065326
This article has not been copyedited and formatted. The final version may differ from this version.

Introduction

Cytochromes P450 (P450) are important enzymes for metabolizing drugs and xenobiotics (Guengerich, 2003). Alteration of their activities through inhibition, inactivation and/or induction can lead to drug-drug interactions (DDI) (Obach et al., 2006; Chu et al., 2009; Grimm et al., 2009). DDI can result in increasing variability of drug exposure in the patient population, the need for dose adjustment to ensure safe and efficacious therapeutic doses (Ogu and Maxa, 2000), and/or can lead to severe adverse events, such as torsades de pointes as observed with terfenidine (Honig et al., 1993). A central component in providing more predictive models of DDI involving enzyme inactivators and/or inducers (Mayhew et al., 2000;Yamashita et al., 2013), is the degradation rate of P450s. In parallel, regulators are open to applying predictive models of DDI as a viable alternative to conducting clinical studies (Zhao et al., 2011).

The reported turnover half-lives for CYP3A are highly variable (Yang et al., 2008) ranging from 10 to 140h. Both EMA and FDA regulatory guidance documents recognize that k_{deg} values have not been unambiguously determined and recommend that a sensitivity analysis is performed to investigate potential DDI based on *in vitro* time dependent inactivation (FDA, 2012). EMA further recommends the use of an *in vivo* derived k_{deg} value if possible (EMA, 2012). Generating an accurate *in vivo* k_{deg} value has proven difficult in humans (Yang et al., 2008), thus requiring the use of indirect measurements of k_{deg} as a surrogate. These have been measured by following de-induction profiles after rifampicin (Fromm et al., 1996;Yang et al., 2008) or carbamazepine administration (Lai et al., 1978), as well as auto-induction of ritonavir (Hsu et al., 1997) and carbamazepine (Magnusson et al., 2008). Both approaches require the inducer to have a much shorter half-life than the target enzyme. The probe substrate should also have a short half-life and be relatively specific for the enzyme being measured, as multiple

enzymes can be induced by the same nuclear receptor pathway. Attempts have also been made to derive a k_{deg} value from enzyme recovery after inactivation (Yang et al., 2008).

Experimental approaches to determine k_{deg} values have included *in vitro* systems such as human hepatocytes or liver slices. Studies monitoring the apoprotein and activities of several P450s in human liver slices provided initial evidence that there can be differential loss of P450 (Renwick et al., 2000). Caveats in this approach include the assumption that *de novo* enzyme synthesis is not occurring during the assessment of degradation and that loss of cell viability or de-differentiation are not contributing to loss of protein. A number of studies have consistently shown a pronounced loss of hepatic phenotype and enzyme activity for drug metabolizing enzymes (DME) in hepatocytes with time in culture (Hamilton et al., 2001;LeCluyse, 2001;Pichard-Garcia et al., 2002;Rodriguez-Antona et al., 2002). Despite modifications to culturing techniques which have improved viability and stability of hepatocytes, such as addition of extracellular matrix over hepatocytes (sandwich) or use of low levels of dexamethasone, there is still a narrow window of use, with significant and differential loss of DME activity (Hewitt et al., 2007). Human HepatoPac (Khetani and Bhatia, 2008) retains elevated and stable P450 enzyme activity for an extended period of time. This hepatocyte model has been useful for accurate metabolite profiling (Wang et al., 2010) and for predictions with low clearance drugs (Chan et al., 2013). Additionally, HepatoPac has been successfully applied to provide mechanistic insights into the metabolism and disposition of faldaprevir(Li et al., 2014;Ramsden et al., 2014c;Ramsden et al., 2014a).

The ability to maintain P450 enzyme activity over an extended culture period offers the capability to modulate P450 levels by siRNA suppression or induction (Ramsden et al., 2014b). Cytokines, including IL6, can down regulate some P450 isoforms, including CYP3A (Morgan,

1997;Morgan et al., 2008). In this study, both siRNA and IL6 treatments were used to lower CYP3A levels. siRNA and IL6 treatments act by suppressing levels of mRNA, albeit through different mechanisms (Fire et al., 1998;Hammond et al., 2000;Yu, 2007;Morgan, 2001;Morgan et al., 2008). During the decline and recovery phases, accurate k_{deg} values for CYP3A (mRNA and enzyme) were obtained. Since the rate of protein synthesis is dependent on the rate constants of both mRNA and protein (Hargrove and Schmidt, 1989), simultaneously fitting the recovery data allowed for estimation of the synthesis rate for mRNA. This approach should be applicable to directly measure k_{deg} values of other drug metabolizing enzymes for inactivation and induction and also for induction of transporters, for use in DDI predictions.

DMD Fast Forward. Published on June 15, 2015 as DOI: 10.1124/dmd.115.065326
This article has not been copyedited and formatted. The final version may differ from this version.

Materials and Methods

Human HepatoPac cultures and proprietary maintenance and probing media were purchased from Hepregen Corporation (Medford, MA) and cultures were prepared from cryoplateable human hepatocytes purchased from Invitrogen Life Technologies (Grand Island, NY) or CellzDirect, (Research Triangle Park, NC). Human interleukin 6 (IL6) and 1'OHmidazolam were purchased from Sigma Aldrich Inc. (St. Louis, MO). Midazolam was purchased from Cerilliant (Round Rock, TX). Testosterone and 6βOHtestosterone were purchased from Steraloids (Newport, RI). Isotopically labeled internal standards $^{13}C_3$ 1′-hydroxymidazolam and 6βOHtestosterone-d7 were purchased from BD biosciences (San Jose, CA). MagMax total RNA recovery bead kits, RT-PCR, and Taqman low density arrays were purchased from Invitrogen Life Technologies (Grand Island, NY). Dharmacon Smart Pool Accell^{TM} RNAi, non-targeting pools, GAPDH pools and delivery media were purchased from (Thermo Scientific, Lafayette, CO).

Cell Culture

Plateable cryopreserved primary human hepatocytes were purchased from commercial vendors permitted to sell products derived from human organs procured in the United States by federally designated Organ Procurement Organizations. Donor information can be found in Table 1. HepatoPac plates were prepared by the manufacturer as previously described (Khetani and Bhatia, 2008) prior to shipment to Boehringer Ingelheim Pharmaceuticals (BIPI, Ridgefield, CT). Cryopreserved human hepatocytes were seeded with 32,000 (in a 24-well plate) or 5,000 (in a 96-well plate) hepatocytes per well and cultured for 9 days post seeding before initiating experiments. The maintenance medium was supplied by Hepregen and contains 10% bovine serum (hHCM). For incubations, proprietary serum free probing medium supplied by Hepregen,

DMD Fast Forward. Published on June 15, 2015 as DOI: 10.1124/dmd.115.065326
This article has not been copyedited and formatted. The final version may differ from this version.

was used (hHPM). The plates were cultured in an incubator with 10% CO_2 and 99% relative humidity at 37°C. Culture medium was replaced every 2 days (400 µL per 24 well or 64 µL per 96 well) prior to incubation with siRNA, IL6 and probe substrates. HepatoPac cultures were maintained in hHCM with 10% serum for 9 days post seeding prior to siRNA or IL6 treatment.

siRNA treatment

At day 9 post seeding siRNA treatment was initiated. Dharmacon Smart Pool Accell™ RNAi was used at a concentration of 1 µM as outlined in the product kit insert, and as previously described (Ramsden et al., 2014b). At 30 minutes, 24, 48 and 72h after siRNA treatment, cells were washed and enzyme activity was assessed under linear time point conditions.

IL6 treatment

At day 9 post seeding IL6 treatments were initiated. IL6 was prepared to the desired incubation concentration in hHCM containing 10% bovine serum. Solutions containing IL6 were refreshed daily (400 µL per 24 well or 64 µL per 96 well). Enzyme activity was determined by removing hHCM containing IL6 and washing the cells once with hHPM as described. Using an ELISA kit (Sigma Aldrich, St. Louis, MO) to measure IL6 levels the concentrations of IL6 were maintained over the length of the dosing period (data not shown).

Enzyme activity assessment

P450 activity was measured as metabolite production, by *in situ* incubation of probe substrates with hepatocyte cultures at 37ºC with 10% CO_2. Probe substrate solution (midazolam or testosterone for CYP3A4) was prepared at 200-fold the desired final concentration in methanol and added to serum free medium. Total concentration of solvent did not exceed 1%. Wells containing the hepatocyte cultures were washed with serum free medium (64 µL for a 96-well plate or 400 µL for a 24-well plate) prior to substrate incubation. After washing, medium

DMD Fast Forward. Published on June 15, 2015 as DOI: 10.1124/dmd.115.065326
This article has not been copyedited and formatted. The final version may differ from this version.

was aspirated and reactions were initiated by adding the same volume of medium containing probe substrate. Substrates were generally incubated at concentrations achieving V_{max} [testosterone (200 µM)]. Midazolam was incubated at a concentration of 15 µM, since midazolam can exhibit substrate inhibition kinetics at higher concentrations *in vitro* (Giragossian et al., 2009). Initial studies were performed using 24-well plates and the methods were transferred to 96 well plates. There was no difference between enzyme activities determined between plating formats (data not shown). During the recovery leg siRNA treatments (from donor 4) were removed and replaced with proprietary human HepatoPac culture medium containing 10% serum (hHCM). Substrate incubations were performed daily or every other day until recovery was observed. Utilizing a 24-well plate format, multiple time-points were evaluated by removing a 50 µL aliquot at designated time points between 2.5 and 30 minutes and quenching the aliquot with 100 µL of reaction termination solutions (described below). When 96-well plates were used, each well represented an individual time point and reactions were terminated at linear time-points, 2 or 3 per substrate, by adding 128 µL of quench solution directly into the well. Reaction termination solutions (60% acetonitrile and 0.1% acetic acid in water) contained isotopically labeled internal standards (0.1 µM).

Enzyme expression

Cells were exposed to IL6 at 1,000 and 10,000 pg/mL (both concentrations shown to maximally knock down CYP3A4 protein in all donors) for 0, 2, 4, 6, 12 and 24 hours. After the incubation, cell lysates were treated with RNAlater® solution (Ambion, Life technologies, Grand Island, NY) and stored at -20 °C until isolation of RNA. Total RNA was isolated from cell lysates using the MAGmax™ bead based system. The relative mRNA levels for specific gene targets were determined by Taqman® Real Time RT-PCR methods, under a two-step assay.

The first step was preparation of cDNA by reverse transcription of 200 ng total RNA. The RNA concentration of each sample was measured in triplicate using a Nanodrop2000 spectrophotometer (Thermo, USA). Comparative (quantitative) PCR assay was conducted using a 7900 Real Time PCR System (Applied Biosystems) and a custom designed Taqman low density array (TLDA) (Ramsden et al., 2014b). Relative mRNA levels were determined from three different donors by combining triplicate samples and analyzing in duplicate (intra-assay variability).

LC/MS Conditions

Samples were analyzed for metabolite production on a 4000 Qtrap (AB Sciex, Thornhill, Ontario, Canada) attached to either a CTC PAL autosampler (Leap Technologies, Carborboro, NC) with Shimadzu or Perkin Elmer pumps or a Waters Acquity UPLC system (Milford, MA). The aqueous mobile phase (A) and organic mobile phase (B) consisted of 95:5 (v/v) water/acetonitrile and 95:5 (v/v) acetonitrile/water, respectively. Both mobile phases contained 0.1% acetic acid. Samples were eluted through Acquity UPLC columns BEH C_{18} 1.7µm, using validated probe substrate analysis methods. The MRM transitions utilized were 305.0→269.0 (6β-hydroxytestosterone); 312.0→276.0 (6β-hydroxytestosterone-d7); 342.0→324.0 (1'-hydroxymidazolam); 347.0→329.0 (1'-hydroxymidazolam-[$^{13}C_3$]), in positive ion mode.

DMD Fast Forward. Published on June 15, 2015 as DOI: 10.1124/dmd.115.065326
This article has not been copyedited and formatted. The final version may differ from this version.

Data analysis and half-life ($t_{1/2}$) calculations

The MS peak areas of metabolites and the internal standards were obtained. The standard curves for metabolite formation were produced by weighted ($1/x^2$) linear regression of analyte to internal standard peak area ratio versus the nominal concentrations of analyte standards.
In order to assess the stability of CYP3A over culture time, rates of formation of 1'OHmidazolam and 6β-OHtestosterone were determined at various time-points. Rates of formation were scaled to $1x10^6$ cells using equation 1.

Equation 1.

$$\textit{In vitro} \text{ formation rate} = \frac{\text{total pmol formed } \textit{in vitro}}{\text{min}} \times \frac{1\times 10^6 \text{hepatocytes}}{\text{\# of hepatocytes per well (5,000 or 35,000)}}$$

Two equations were used in order to derive the degradation rate of CYP3A from the time-course depletion experiment GraphPad Prism 6 (GraphPad Software Inc.; San Diego, CA). In the first approach linear regression was used and the percent of metabolite after IL6 or siRNA treatment relative to the control (untreated) was transformed by taking the natural logarithm (LN). Data were graphed by plotting the LN percent of control remaining on the y-axis and incubation time (h) on the x-axis. Half-life ($t_{1/2}$) values for CYP3A protein, representative of k_{deg}, were derived from the slope (k) of linear regression using Equation 2.

Equation 2.

$$t_{1/2} = -\frac{Ln(2)}{k}$$

The second approach was to fit the data to a non-linear equation using a one phase exponential decay model (Equation 3). Half-life ($t_{1/2}$) values for CYP3A protein, representative of k_{deg}, were derived from the slope (k) of non-linear regression using Equation 2.

DMD Fast Forward. Published on June 15, 2015 as DOI: 10.1124/dmd.115.065326
This article has not been copyedited and formatted. The final version may differ from this version.

Equation 3. $$Y = (Y_0 - Plateau) \times e^{-k*x} + Plateau$$

To estimate the degradation constant of CYP3A from the recovery data, the kinetic data were first analyzed with Equation 4, where V_{syn} refers to the zero-order enzyme synthesis rate, and E is the amount of CYP, which is reflected by enzyme activity.

$$\frac{dE}{dt} = V_{syn} - k_{deg} * E \qquad \text{Equation 4}$$

At steady-state, the rate of enzyme synthesis is equal to enzyme degradation. Thus,

$$V_{syn} = k_{deg} * E_{ss} \qquad \text{Equation 5}$$

where E_{ss} refers to the steady-state enzyme amount, which is equal to the amount of enzyme in the control cells (E_0). Replacing E in Equation 4 with E' (E/E_0, enzyme activity relative to control), Equation 6 can be obtained, which was used to fit to recovery data for k_{deg} estimation.

$$\frac{dE'}{dt} = k_{deg} - k_{deg} * E' \qquad \text{Equation 6}$$

Equations 4-6 only consider the synthesis and degradation of CYP3A enzyme. To also consider the synthesis and degradation of CYP3A mRNA during the recovery process, Equation 7 and 8 were also applied to model the kinetic data.

$$\frac{dRNA}{dt} = V_{syn,RNA} - k_{deg,RNA} * RNA \qquad \text{Equation 7}$$

$$\frac{dE}{dt} = k_{syn} * RNA - k_{deg} * E \qquad \text{Equation 8}$$

In Equation 7 and 8, $V_{syn,RNA}$, $k_{deg,RNA,}$ and RNA refer to the zero-order synthesis rate, degradation constant, and the amount of CYP3A mRNA, respectively. It was assumed that the CYP3A enzyme synthesis rate is proportional to the amount of mRNA. The k_{syn} in Equation 8 refers to the CYP3A enzyme synthesis rate constant.

DMD Fast Forward. Published on June 15, 2015 as DOI: 10.1124/dmd.115.065326
This article has not been copyedited and formatted. The final version may differ from this version.

At steady-state, the synthesis rate is equal to the degradation rate for both mRNA and enzyme. Thus,

$V_{syn,RNA} = k_{deg,RNA} * RNA_0$ Equation 9

$k_{syn} = k_{deg} * E_0 / RNA_0$ Equation 10

Combining Equation 7 and 8 with Equation 9 and 10 and replacing RNA and E in Equation 7 and 8 with RNA'(RNA/RNA_0, the amount of RNA relative to control) and E'(E/E_0, enzyme activity relative to control), Equation 11and 12 can be obtained.

$\frac{dRNA'}{dt} = k_{deg,RNA} - k_{deg,RNA} * RNA'$ Equation 11

$\frac{dE'}{dt} = k_{deg} * RNA' - k_{deg} * E'$ Equation 12

The enzyme recovery kinetic data were analyzed with Equation 11 and 12, assuming k_{deg} =0.0316 h^{-1} (estimated with the depletion approach for donor 4) for $k_{deg,RNA}$ estimation or assuming $k_{deg,RNA}$=0.0282 h^{-1} (Yamashita et al., 2013) for $k_{deg,}$ estimation. Kinetic analysis for enzyme recovery was performed with ADAPT5 (version 5.0.48, Los Angeles, California).

DMD Fast Forward. Published on June 15, 2015 as DOI: 10.1124/dmd.115.065326
This article has not been copyedited and formatted. The final version may differ from this version.

Results

Stability and reproducibility of CYP3A enzyme activity. To determine whether the HepatoPac model maintained appropriate and constant levels of CYP3A over the treatment period, the longevity and reproducibility of enzyme activity was monitored. Markers of CYP3A activity included both testosterone 6βhydroxylation, Graph A (Figure 1) and midazolam 1'hydroxylation, Graph B (Figure 1). Using two separate preparations of the same donor hepatocytes, enzyme activity was captured at time points spanning 28 days in culture. A one-way ANOVA test was run against all measurements using GraphPad Prism v6 and indicated that there was no statistical difference between repeat measurements determined on different days. Additionally, the percent difference between measurements was calculated by comparing the rates on each day with the rates determined from the measurement before. This analysis, Graph C showed that there was a >40% difference between Day 7 and Day 8 measurements (capturing the acclimation time) and also a >40% difference in two out of four measured activities between Day 20 and Day 24 or Day 24 and Day 28, all other data points fell within 20%. Based on these observations CYP3A activity was confirmed to be stable up to Day 20-24 (Figure 1).

Impact of IL6 treatment on multiple DME gene targets. In order to confirm that IL6 works through depletion of mRNA levels, a handful of DME gene targets, previously shown to be modulated by IL6, were analyzed after various time points of exposure. Levels of CYP2C9, CYP3A4, UGT1A1, ABCB1 and SLCO1B1 followed similar rates of decline after exposure to IL6 (Figure 2), in contrast the house-keeping gene GAPDH did not show any change in level upon addition of IL6. The estimated half-life value determined from the three time-points before complete loss of CYP3A4 mRNA was observed was 1.9h.

DMD Fast Forward. Published on June 15, 2015 as DOI: 10.1124/dmd.115.065326
This article has not been copyedited and formatted. The final version may differ from this version.

Enzyme activity of CYP3A during exposure to IL6. CYP3A enzyme activity was determined after exposure to IL6 for 24, 48, 72 and 96 hours, in five different donors (demographics in Table 1). Treatment of all donors with 1,000 or 10,000 pg/mL IL6 resulted in time dependent loss of CYP3A activity with total loss in activity occurring by 96 hours. The percent of activity remaining at each time point was fit to linear and non-linear regression models as presented in Figure 3. The average half-life for CYP3A activity and corresponding degradation rate for each donor is presented in Table 3. The average rate of degradation determined by this method was $0.0240 \pm 0.005\ h^{-1}$.

Recovery of CYP3A4 after IL6 treatment. The kinetic data for CYP3A enzyme recovery upon removal of 1,000 pg/mL or 10,000 pg/mL of IL6 were first analyzed with a model which considers only the synthesis and degradation of CYP3A enzyme. The initial CYP3A4 enzyme level immediately after removal of 1,000 pg/mL and 10,000pg/mL of IL6 treatment were determined to be 7.4% and 3.6% of the control, respectively. These initial state conditions were used in model fitting and the results are shown in Figures 4A, 4B, and Table 4. By visual inspection of the simulated vs observed data, the data, especially early time-points, were not well-recovered by the model. In addition, the estimated k_{deg} values were 0.0131 and $0.0111\ h^{-1}$, which were more than 2-fold lower than the k_{deg} value estimated using the enzyme depletion approach ($k_{deg} = 0.0316\ h^{-1}$ for donor 4). Both observations suggested that this model (Equation 6) was not a good model to explain the CYP3A enzyme recovery after removal of IL6 treatment. To capture these dynamics, a model which considers the synthesis and degradation of both CYP3A mRNA and enzyme (Equation 11 and 12) was fit to the enzyme recovery kinetic data. The initial CYP3A mRNA levels, after removal of 1,000 pg/mL and 10,000 pg/mL of IL6, were both assumed to be 0. The initial CYP3A enzyme levels, after removal of 1,000 pg/mL and

DMD Fast Forward. Published on June 15, 2015 as DOI: 10.1124/dmd.115.065326
This article has not been copyedited and formatted. The final version may differ from this version.

10,000 pg/mL of IL6, were as previously described. The model fitting results, with these initial state conditions, are shown in Figures 4C, 4D, and Table 5. Because CYP3A mRNA levels at different recovery time points were not determined, $k_{deg,RNA}$ and k_{deg} could not both be estimated using only the CYP3A enzyme recovery data.

Using the k_{deg} value determined with the depletion method (k_{deg} = 0.0316 h^{-1} for donor 4), the CYP3A mRNA degradation constant ($k_{deg,RNA}$) was estimated to be 0.0296 h^{-1} and 0.0213 h^{-1} after removal of 1,000 pg/mL and 10,000 pg/mL of treatment, respectively. These values were close to the reported CYP3A mRNA degradation constant (0.0282 h^{-1}) (Yamashita et al., 2013). Using this literature reported $k_{deg,RNA}$ (0.0282 h^{-1}), the degradation constant of CYP3A enzyme (k_{deg}) was estimated to 0.0335h^{-1} and 0.0231 h^{-1} for removal of 1,000 pg/mL and 10,000 pg/mL of treatment, respectively, which are also close to the CYP3A enzyme degradation constant determined with the depletion approach (0.0316 h^{-1} for donor 4). By visually comparing the observed vs simulated data and also comparing the AIC values for both models, the model (Equation 9 and 10) which considers the synthesis and degradation of both CYP3A mRNA and enzyme was considered to be a better model for CYP3A recovery upon removal of IL-6 than the model considering only the synthesis and degradation of CYP3A enzyme (Equation 6).

Comparison of IL6 and siRNA treatment on derivation of CYP3A4 degradation rate. In one donor a comparison was made between the degradation rates calculated after siRNA targeting CYP3A4 or IL6 treatment (10,000 pg/mL). Both methods resulted in comparable rates of degradation, 0.0322 h^{-1} for siRNA compared with 0.0383 h^{-1} for IL6 (Figure 5).

DMD Fast Forward. Published on June 15, 2015 as DOI: 10.1124/dmd.115.065326
This article has not been copyedited and formatted. The final version may differ from this version.

Discussion

Various methods for predicting DDI with enzyme inactivators have been developed, including both static and semi-physiological models (Galetin et al., 2006;Grimm et al., 2009;Obach et al., 2007;Einolf, 2007;Fenneteau et al., 2010;Quinney et al., 2010), each relying on k_{deg} for the enzyme as a key input parameter. As physiologically based pharmacokinetic modeling is more routinely applied to predict complex drug interactions, many researchers have noted improved prediction accuracy when using a CYP3A k_{deg} of 0.03 h^{-1}(Friedman et al., 2011;Wang, 2010;Yamashita et al., 2013), determined from the time-course of CYP3A recovery following multiple-dose clarithromycin administration. The current approach, which resulted in an overall CYP3A k_{deg} of 0.0240 h^{-1}, relied on human hepatocytes, specifically the human HepatoPac model, as a viable *in vitro* surrogate of CYP regulation. Studies from our labs and others have characterized the activity, longevity and functionality of the HepatoPac model (Chan et al., 2013;Davidson et al., 2014;Khetani and Bhatia, 2008;Ramsden et al., 2014b;Wang et al., 2010). We have reproducibly observed stable CYP3A activity over 2.5 weeks after stabilization. Taking advantage of the long-term stability of CYP3A in this model, as measured by testosterone and midazolam hydroxylation (Figure 1), and assuming that the changes in enzyme activity reflect degradation of the CYP3A4 protein CYP3A4 levels were modulated with siRNA and IL6 treatment resulting in a >90% loss of mRNA (Figure 2) at 6h and undetectable levels at time points after 6h. There was concomitant loss (~98%) of enzyme activity (Figure 3). The estimated half-life for CYP3A4 mRNA degradation, in the presence of IL6, was 1.9h, with total loss (>90%) observed by 6h.

The longevity of the HepatoPac model enabled a recovery leg such that, upon removal of IL6 treatment (1,000 or 10,000 pg/mL), CYP3A enzyme activity returned to baseline levels

DMD Fast Forward. Published on June 15, 2015 as DOI: 10.1124/dmd.115.065326
This article has not been copyedited and formatted. The final version may differ from this version.

(Figure 4). Since the mechanism behind IL6 mediated suppression of CYP3A is by depletion of mRNA levels, it was not surprising that the kinetic data for CYP3A enzyme recovery fitted better to the model which considered recovery of both CYP3A mRNA and protein. When the degradation value of 0.0316 h^{-1} was used to project the rate of mRNA synthesis (and degradation), after removal of IL6, $k_{deg,RNA}$ was estimated to be 0.0296 h^{-1} and 0.0213 h^{-1} for removal of 1,000 and 10,000 pg/mL ,respectively, which are consistent with a previously reported CYP3A mRNA degradation constant of 0.0282 h^{-1} (Yamashita et al., 2013). The longevity of HepatoPac cultures should also lend themselves to the conduct of pulse-chase experiments as a fundamental approach to determine protein degradation (Zhou, 2004).

A similar treatment regimen (siRNA) has been used to effectively suppress CYP3A4 levels in order to evaluate possible protein-protein interactions between CYP2C9 and CYP3A4 (Ramsden et al., 2014b). In this model, CYP2C9 activity increased upon lowering of CYP3A4 levels and then returned to pre-treatment activities following restoration of CYP3A4 levels (after removal of siRNA). These experimental paradigms suggest that normal regulatory control of P450 expression is occurring in the HepatoPac cultures.

The degradation value of 0.0240 h^{-1} for CYP3A4, representing a $t_{1/2}$ of 29h, is in agreement with values obtained by Yang et al. 2008 (26h) using data generated in hepatocytes and liver slices. Additionally, improved prediction accuracy has been noted using a similar k_{deg} value in PBPK modeling (0.03 h^{-1}) (Friedman et al., 2011;Quinney et al., 2010;Wang, 2010;Yamashita et al., 2013). As discussed in detail by Yang et al (2008), a number of approaches have been applied to estimate half-life of P450 degradation. Half-life values obtained by these methods include following clinical markers of P450 activity such as 6β-hydroxy cortisol formation during induction (72h; (Tran et al., 1999), *in vivo* mechanism based

inhibition of CYP2D6 by paroxitene, as assessed by dextromethorphan metabolism (51h; (Venkatakrishnan and Obach, 2005), and in human hepatocytes assessing CYP1A2 by de-induction (51h; (Diaz et al., 1990).

In the current study, k_{deg} was determined by direct measurement in hepatocytes from 5 human donors, which provided a range of $t_{1/2}$ values from 22-39h with a calculated mean value of 29h. A possible contributor to the variability in the k_{deg} value for CYP3A is the variable contribution of CYP3A5 to enzyme activity, depending on the donor phenotype. The hepatocytes used in the current study were determined to be representative of the overall population with respect to CYP3A5 expression. There is evidence that IL6 can also effectively reduce CYP3A5 levels (Dickmann et al., 2011). In contrast, CYP3A4 siRNA specifically targets CYP3A4 and hence CYP3A5, if active, would not be down-regulated. Genotyping of donors 2, 3 and 5 was performed which indicated that only donor 2 expressed CYP3A5 (*1*3). There is a strong correlation between genotype and phenotype of CYP3A5 (Lin et al., 2002). CYP3A4 and CYP3A5 have overlapping substrate specificities (Lamba et al., 2002) and both enzymes can produce 1'OH-midazolam from incubations with midazolam. CYP3A5 expression is highly variable in humans, with readily detectable levels in 25 to 30% of the population and very low or undetectable levels in the remainder (Wrighton et al., 1990;Wrighton et al., 2000;Paine et al., 1997). In these studies, there was clearly a longer $t_{1/2}$ from donor 2, where there may be an overlapping contribution of CYP3A5 to the formation of 1'OH midazolam (Table 3). Donors 3 and 5 did not have functional CYP3A5 (*3*3), and the half-life values of CYP3A were 32.3 and 25.2, respectively. Using the genotyping information, the CYP3A4 specific $t_{1/2}$ was determined to be 27.2 ± 5 h upon removal of donor 2. In donor 4, where comparisons were made between both approaches to suppress CYP3A4, genotyping studies were

not performed to determine whether this donor expressed active CYP3A5 (*1*1 or *1*3). There was no significant variation in the degradation rate obtained for donor 4 using both methods (0.0322 h^{-1}, IL6 and 0.0383 h^{-1}, siRNA) suggesting that CYP3A5 is not a major component of overall CYP3A content in this individual (Figure 5). CYP3A5 *1*1 has a low frequency (~1.7%) and was not evaluated during these studies.

Typically studies evaluating mechanism based inhibition use pooled HLM which represent the overall population (Grimm et al., 2009;Obach et al., 2007). As such, inactivation parameters do not differentiate between CYP3A4 and CYP3A5. Similarly, when predicting clinical outcomes for CYP3A substrates, such as midazolam, the effect on the overall population is determined rather than the relative effects on CYP3A4 and CYP3A5. Since the hepatocyte donors used to derive the $t_{1/2}$ and k_{deg} values in this study are representative of the overall population (~20% CYP3A5 expressors), the recommendation from these data is to use the CYP3A population k_{deg} value of 0.0240 h^{-1}. This value will cover the degradation rate for ~99% of the population.

It is thought that IL6 modulates mRNA levels through a receptor mediated cascade while siRNA directly targets mRNA levels (Elbashir et al., 2001;Morgan et al., 2008;Scherr et al., 2003) although the possibility that IL6 may affect the rate of protein degradation in ways other than mRNA down regulation cannot be excluded. Both methods rapidly reduce mRNA levels. Hence, the rate of protein degradation is the rate limiting step. Therefore, the loss of enzyme activity observed over time should be reflective of the half-life of the protein being measured. An advantage of the current approach is that the degradation rate was determined in the absence of protein re-synthesis, due to the presence of IL6 and siRNA. Additionally, the degradation and synthesis rates for CYP3A4 were calculated using a more direct route of measurement,

independent of half-life of substrate or inducing agents, using an *in vitro* system capable of maintaining long-term normal regulatory control of P450 expression.

An accurate measurement of k_{deg} should enable researchers to systematically evaluate the accuracy of predictions for drug-drug interaction potential such as those mediated by mechanism based inactivators. Both Galetin et al. (2006) and Wong (2011) provided insightful summaries of why there are differences in predictability between models. Galetin et al. (2006) summarized the caveats of *in vitro* models of TDI which yielded large variability in estimating kinetic parameters, K_I and k_{inact}. The studies showed the best prediction when using inhibitor input values of C_{avg} and a $t_{1/2}$ for CYP3A4 of 72h (89% within 2-fold). This is much longer than the $t_{1/2}$ value obtained in our studies (29 ± 7h). In his review, Wong (2011) effectively summarized the need for systematic evaluation of each parameter which suggested that accurate predictions could be obtained by modifying which inhibitor concentration was selected, in addition to which degradation rate was used. Many researchers have adopted a value of 0.019 h^{-1} (36h) for hepatic k_{deg} (Obach et al., 2007). This value determined through indirect measurement, from the kinetics of induction and de-induction of verapamil oral clearance by rifampin (Fromm et al., 1996) is close to the value determined in our studies. Other researchers have resorted to using pairs of k_{deg} values to bracket potential clinical changes (Minematsu et al., 2010). Having a better estimate of k_{deg}, may enable systematic evaluation of the other input values used for predicting drug-drug interaction potential.

ACKNOWLEDGMENTS

The authors would like to thank Drs Timothy S. Tracy, Yongmei Li and Hongbin Yu for thoughtful discussions and scientific advice. The authors would like to thank Dr. Patrick Baum for genotyping the HepatoPac donors and Dr. Tom S. Chan for analyzing IL6 levels. Lastly, the authors would like to thank Drs Swati Nagar and Kenneth R. Korzekwa for critically reviewing the manuscript.

AUTHORSHIP CONTRIBUTIONS

Participated in research design: Ramsden and Tweedie

Conducted experiments: Ramsden

Performed data analysis: Ramsden and Zhou

Wrote or contributed to the writing of the manuscript: Ramsden, Zhou and Tweedie

DMD Fast Forward. Published on June 15, 2015 as DOI: 10.1124/dmd.115.065326
This article has not been copyedited and formatted. The final version may differ from this version.

Reference List

Chan T, Yu H, Moore A, Khetani S and Tweedie D J (2013) Meeting the Challenge of Predicting Hepatic Clearance of Compounds Slowly Metabolized by Cytochrome P450 Using a Novel Hepatocyte Model, HepatoPacTM. *Drug Metab Dispos*.

Davidson MD, Lehrer M and Khetani S R (2014) Hormone and Drug-Mediated Modulation of Glucose Metabolism in a Microscale Model of the Human Liver. *Tissue Eng Part C Methods*.

Diaz D, Fabre I, Daujat M, Saint A B, Bories P, Michel H and Maurel P (1990) Omeprazole Is an Aryl Hydrocarbon-Like Inducer of Human Hepatic Cytochrome P450. *Gastroenterology* **99**:737-747.

Dickmann LJ, Patel S K, Rock D A, Wienkers L C and Slatter J G (2011) Effects of Interleukin-6 (IL-6) and an Anti-IL-6 Monoclonal Antibody on Drug-Metabolizing Enzymes in Human Hepatocyte Culture. *Drug Metab Dispos* **39**:1415-1422.

Einolf HJ (2007) Comparison of Different Approaches to Predict Metabolic Drug-Drug Interactions. *Xenobiotica* **37**:1257-1294.

Elbashir SM, Harborth J, Lendeckel W, Yalcin A, Weber K and Tuschl T (2001) Duplexes of 21-Nucleotide RNAs Mediate RNA Interference in Cultured Mammalian Cells. *Nature* **411**:494-498.

EMA. European Medicines Agency; Committee for Human Medicinal Products (CHMP);Guideline on the Investigation of Drug interactions. 6-21-2012. 9-13-0013.
Ref Type: Online Source

FDA. Guidance for Industry: Drug Interaction Studies-Study Design, Data Analysis, Implications for Dosing and Labeling Recommendations (Draft). 2012. 9-13-0013.
Ref Type: Online Source

Fenneteau F, Poulin P and Nekka F (2010) Physiologically Based Predictions of the Impact of Inhibition of Intestinal and Hepatic Metabolism on Human Pharmacokinetics of CYP3A Substrates. *J Pharm Sci* **99**:486-514.

Fire A, Xu S, Montgomery M K, Kostas S A, Driver S E and Mello C C (1998) Potent and Specific Genetic Interference by Double-Stranded RNA in Caenorhabditis Elegans. *Nature* **391**:806-811.

Friedman EJ, Fraser I P, Wang Y H, Bergman A J, Li C C, Larson P J, Chodakewitz J, Wagner J A and Stoch S A (2011) Effect of Different Durations and Formulations of Diltiazem on the Single-Dose Pharmacokinetics of Midazolam: How Long Do We Go? *J Clin Pharmacol* **51**:1561-1570.

Fromm MF, Busse D, Kroemer H K and Eichelbaum M (1996) Differential Induction of Prehepatic and Hepatic Metabolism of Verapamil by Rifampin. *Hepatology* **24**:796-801.

Galetin A, Burt H, Gibbons L and Houston J B (2006) Prediction of Time-Dependent CYP3A4 Drug-Drug Interactions: Impact of Enzyme Degradation, Parallel Elimination Pathways, and Intestinal Inhibition. *Drug Metab Dispos* **34**:166-175.

Giragossian C, LaPerle J, Kosa R E and Gillian S (2009) Impact of Time-Dependent Inactivation on the Estimation of Enzyme Kinetic Parameters for Midazolam. *Drug Metab Lett* **3**:45-53.

Grimm SW, Einolf H J, Hall S D, He K, Lim H K, Ling K H, Lu C, Nomeir A A, Seibert E, Skordos K W, Tonn G R, Van H R, Wang R W, Wong Y N, Yang T J and Obach R S (2009) The Conduct of in Vitro Studies to Address Time-Dependent Inhibition of Drug-Metabolizing Enzymes: a Perspective of the Pharmaceutical Research and Manufacturers of America. *Drug Metab Dispos* **37**:1355-1370.

Guengerich FP (2003) Cytochromes P450, Drugs, and Diseases. *Mol Interv* **3**:194-204.

Hamilton GA, Jolley S L, Gilbert D, Coon D J, Barros S and LeCluyse E L (2001) Regulation of Cell Morphology and Cytochrome P450 Expression in Human Hepatocytes by Extracellular Matrix and Cell-Cell Interactions. *Cell Tissue Res* **306**:85-99.

Hammond SM, Bernstein E, Beach D and Hannon G J (2000) An RNA-Directed Nuclease Mediates Post-Transcriptional Gene Silencing in Drosophila Cells. *Nature* **404**:293-296.

Hargrove JL and Schmidt F H (1989) The Role of MRNA and Protein Stability in Gene Expression. *FASEB J* **3**:2360-2370.

Hewitt NJ, Lechon M J, Houston J B, Hallifax D, Brown H S, Maurel P, Kenna J G, Gustavsson L, Lohmann C, Skonberg C, Guillouzo A, Tuschl G, Li A P, LeCluyse E, Groothuis G M and Hengstler J G (2007) Primary Hepatocytes: Current Understanding of the Regulation of Metabolic Enzymes and Transporter Proteins, and Pharmaceutical Practice for the Use of Hepatocytes in Metabolism, Enzyme Induction, Transporter, Clearance, and Hepatotoxicity Studies. *Drug Metab Rev* **39**:159-234.

Hsu A, Granneman G R, Witt G, Locke C, Denissen J, Molla A, Valdes J, Smith J, Erdman K, Lyons N, Niu P, Decourt J P, Fourtillan J B, Girault J and Leonard J M (1997) Multiple-Dose Pharmacokinetics of Ritonavir in Human Immunodeficiency Virus-Infected Subjects. *Antimicrob Agents Chemother* **41**:898-905.

Khetani SR and Bhatia S N (2008) Microscale Culture of Human Liver Cells for Drug Development. *Nat Biotechnol* **26**:120-126.

Lai AA, Levy R H and Cutler R E (1978) Time-Course of Interaction Between Carbamazepine and Clonazepam in Normal Man. *Clin Pharmacol Ther* **24**:316-323.

Lamba JK, Lin Y S, Schuetz E G and Thummel K E (2002) Genetic Contribution to Variable Human CYP3A-Mediated Metabolism. *Adv Drug Deliv Rev* **54**:1271-1294.

LeCluyse EL (2001) Human Hepatocyte Culture Systems for the in Vitro Evaluation of Cytochrome P450 Expression and Regulation. *Eur J Pharm Sci* **13**:343-368.

Li Y, Zhou J, Ramsden D, Taub M E, O'Brien D, Xu J, Busacca C A, Gonnella N and Tweedie D J (2014) Enzyme-Transporter Interplay in the Formation and Clearance of Abundant Metabolites of Faldaprevir Found in Excreta but Not in Circulation. *Drug Metab Dispos* **42**:384-393.

Lin YS, Dowling A L, Quigley S D, Farin F M, Zhang J, Lamba J, Schuetz E G and Thummel K E (2002) Co-Regulation of CYP3A4 and CYP3A5 and Contribution to Hepatic and Intestinal Midazolam Metabolism. *Mol Pharmacol* **62**:162-172.

Magnusson MO, Dahl M L, Cederberg J, Karlsson M O and Sandstrom R (2008) Pharmacodynamics of Carbamazepine-Mediated Induction of CYP3A4, CYP1A2, and Pgp As Assessed by Probe Substrates Midazolam, Caffeine, and Digoxin. *Clin Pharmacol Ther* **84**:52-62.

Mayhew BS, Jones D R and Hall S D (2000) An in Vitro Model for Predicting in Vivo Inhibition of Cytochrome P450 3A4 by Metabolic Intermediate Complex Formation. *Drug Metab Dispos* **28**:1031-1037.

Minematsu T, Lee J, Zha J, Moy S, Kowalski D, Hori K, Ishibashi K, Usui T and Kamimura H (2010) Time-Dependent Inhibitory Effects of (1R,9S,12S,13R,14S,17R,18E,21S,23S,24R,25S,27R)-1,14-Dihydroxy-12-(E)-2-[(1R,3R,4 R)-4-Hydroxy-3-Methoxycyclohexyl]-1-Methylvinyl-23,25-Dimethoxy-13,19,21,27-Tetra Methyl-17-(2-Oxopropyl)-11,28-Dioxa-4-Azatricyclo[22.3.1.0(4.9)]Octacos-18-Ene-2, 3,10,16-Tetrone (FK1706), a Novel Nonimmunosuppressive Immunophilin Ligand, on CYP3A4/5 Activity in Humans in Vivo and in Vitro. *Drug Metab Dispos* **38**:249-259.

Morgan ET (1997) Regulation of Cytochromes P450 During Inflammation and Infection. *Drug Metab Rev* **29**:1129-1188.

Morgan ET (2001) Regulation of Cytochrome P450 by Inflammatory Mediators: Why and How? *Drug Metab Dispos* **29**:207-212.

Morgan ET, Goralski K B, Piquette-Miller M, Renton K W, Robertson G R, Chaluvadi M R, Charles K A, Clarke S J, Kacevska M, Liddle C, Richardson T A, Sharma R and Sinal C J (2008) Regulation of Drug-Metabolizing Enzymes and Transporters in Infection, Inflammation, and Cancer. *Drug Metab Dispos* **36**:205-216.

Obach RS, Walsky R L and Venkatakrishnan K (2007) Mechanism-Based Inactivation of Human Cytochrome P450 Enzymes and the Prediction of Drug-Drug Interactions. *Drug Metab Dispos* **35**:246-255.

Ogu CC and Maxa J L (2000) Drug Interactions Due to Cytochrome P450. *Proc (Bayl Univ Med Cent)* **13**:421-423.

Paine MF, Khalighi M, Fisher J M, Shen D D, Kunze K L, Marsh C L, Perkins J D and Thummel K E (1997) Characterization of Interintestinal and Intraintestinal Variations in Human CYP3A-Dependent Metabolism. *J Pharmacol Exp Ther* **283**:1552-1562.

Pichard-Garcia L, Gerbal-Chaloin S, Ferrini J B, Fabre J M and Maurel P (2002) Use of Long-Term Cultures of Human Hepatocytes to Study Cytochrome P450 Gene Expression. *Methods Enzymol* **357**:311-321.

Quinney SK, Zhang X, Lucksiri A, Gorski J C, Li L and Hall S D (2010) Physiologically Based Pharmacokinetic Model of Mechanism-Based Inhibition of CYP3A by Clarithromycin. *Drug Metab Dispos* **38**:241-248.

Ramsden D, Tweedie D J, Chan T S, Taub M E and Li Y (2014a) Bridging in Vitro and in Vivo Metabolism and Transport of Faldaprevir in Human Using a Novel Cocultured Human Hepatocyte System, HepatoPac. *Drug Metab Dispos* **42**:394-406.

Ramsden D, Tweedie D J, Chan T S and Tracy T S (2014b) Altered CYP2C9 Activity Following Modulation of CYP3A4 Levels in Human Hepatocytes: an Example of Protein-Protein Interactions. *Drug Metab Dispos* **42**:1940-1946.

Ramsden D, Tweedie D J, St G R, Chen L Z and Li Y (2014c) Generating an in Vitro-in Vivo Correlation for Metabolism and Liver Enrichment of a Hepatitis C Virus Drug, Faldaprevir, Using a Rat Hepatocyte Model (HepatoPac). *Drug Metab Dispos* **42**:407-414.

Renwick AB, Watts P S, Edwards R J, Barton P T, Guyonnet I, Price R J, Tredger J M, Pelkonen O, Boobis A R and Lake B G (2000) Differential Maintenance of Cytochrome P450 Enzymes in Cultured Precision-Cut Human Liver Slices. *Drug Metab Dispos* **28**:1202-1209.

Rodriguez-Antona C, Donato M T, Boobis A, Edwards R J, Watts P S, Castell J V and Gomez-Lechon M J (2002) Cytochrome P450 Expression in Human Hepatocytes and Hepatoma Cell Lines: Molecular Mechanisms That Determine Lower Expression in Cultured Cells. *Xenobiotica* **32**:505-520.

Scherr M, Morgan M A and Eder M (2003) Gene Silencing Mediated by Small Interfering RNAs in Mammalian Cells. *Curr Med Chem* **10**:245-256.

Tran JQ, Kovacs S J, McIntosh T S, Davis H M and Martin D E (1999) Morning Spot and 24-Hour Urinary 6 Beta-Hydroxycortisol to Cortisol Ratios: Intraindividual Variability and Correlation Under Basal Conditions and Conditions of CYP 3A4 Induction. *J Clin Pharmacol* **39**:487-494.

Venkatakrishnan K and Obach R S (2005) In Vitro-in Vivo Extrapolation of CYP2D6 Inactivation by Paroxetine: Prediction of Nonstationary Pharmacokinetics and Drug Interaction Magnitude. *Drug Metab Dispos* **33**:845-852.

Wang WW, Khetani S R, Krzyzewski S, Duignan D B and Obach R S (2010) Assessment of a Micropatterned Hepatocyte Coculture System to Generate Major Human Excretory and Circulating Drug Metabolites. *Drug Metab Dispos* **38**:1900-1905.

Wang YH (2010) Confidence Assessment of the Simcyp Time-Based Approach and a Static Mathematical Model in Predicting Clinical Drug-Drug Interactions for Mechanism-Based CYP3A Inhibitors. *Drug Metab Dispos* **38**:1094-1104.

Wrighton SA, Brian W R, Sari M A, Iwasaki M, Guengerich F P, Raucy J L, Molowa D T and Vandenbranden M (1990) Studies on the Expression and Metabolic Capabilities of Human Liver Cytochrome P450IIIA5 (HLp3). *Mol Pharmacol 1990 Aug;38(2):* **38**:207-213.

Wrighton SA, Schuetz E G, Thummel K E, Shen D D, Korzekwa K R and Watkins P B (2000) The Human CYP3A Subfamily: Practical Considerations. *Drug Metab Rev* **32**:339-361.

Yamashita F, Sasa Y, Yoshida S, Hisaka A, Asai Y, Kitano H, Hashida M and Suzuki H (2013) Modeling of Rifampicin-Induced CYP3A4 Activation Dynamics for the Prediction of Clinical Drug-Drug Interactions From in Vitro Data. *PLoS One* **8**:e70330.

Yang J, Liao M, Shou M, Jamei M, Yeo K R, Tucker G T and Rostami-Hodjegan A (2008) Cytochrome P450 Turnover: Regulation of Synthesis and Degradation, Methods for Determining Rates, and Implications for the Prediction of Drug Interactions. *Curr Drug Metab* **9**:384-394.

Yu AM (2007) Small Interfering RNA in Drug Metabolism and Transport. *Curr Drug Metab* **8**:700-708.

Zhao P, Zhang L, Grillo J A, Liu Q, Bullock J M, Moon Y J, Song P, Brar S S, Madabushi R, Wu T C, Booth B P, Rahman N A, Reynolds K S, Gil B E, Lesko L J and Huang S M (2011) Applications of Physiologically Based Pharmacokinetic (PBPK) Modeling and Simulation During Regulatory Review. *Clin Pharmacol Ther* **89**:259-267.

Zhou P (2004) Determining Protein Half-Lives. *Methods Mol Biol* **284**:67-77.

Legends for Figures

Figure 1: Stability of CYP3A enzyme activity over time in donor 3. Each experiment included n=4 data points for each time-point. Measurements of Graph B, 1'OH midazolam and Graph A, 6'βOH testosterone were used as a marker of CYP3A activity under linear time conditions. Graph C shows the % difference between rates of formation between days. One-way Anova testing determined no significant difference between repeat data points. Visibly the activity decreased at some points on Days 24 and Day 28.

Figure 2: Impact of IL6 treatment on mRNA levels. Data represent mean values from n=2 donor treatments, each containing (3 inter-assay pooled replicates and 2 intra-assay replicates). Graph A shows decreases in mRNA levels for a handful of drug metabolizing targets shown in literature to be down-regulated by IL-6. GAPDH levels were measured as a negative control. Graph B shows the natural logarithm of the percent of CYP3A4 control which was used to calculate the half-life.

Figure 3: CYP3A activity in 5 human donors, measured by 1'OH midazolam formation n=3 per treatment time), total n=6 (n =3, 1,000 and n=3, 10,000 pg/mL IL6). Activity is expressed as a percentage of the untreated control (0 pg/mL IL6). Graph A, natural logarithm of the percent of control. The slope of the loss of enzyme activity was used to calculate the half-life ($\frac{-Ln\,(2)}{slope}$), which is equal to the rate of degradation. Graph B, one phase exponential decay equation using the mean and standard deviations generated from donors 1, 2, 3, 4 and 5.

Figure 4: Modeling of CYP3A enzyme recovery data upon removal of IL6 using Equation 6 (A and B) or Equation 10 and 11 (C and D). Lines represent simulated profiles; filled circles are observed data.

Figure 5: Comparison of half-life values obtained between siRNA and IL6 treatments in donor 4. CYP3A activity measured by 1'OH midazolam formation n=3 per treatment time course. The natural logarithm of percent of 0 pg/ml IL6 treatment was applied to derive the slope for calculation the half-life of enzyme activity, which is equal to the rate of degradation. The axis on the inset graph is split so that the earlier time-point for siRNA activity can be visualized.

DMD Fast Forward. Published on June 15, 2015 as DOI: 10.1124/dmd.115.065326
This article has not been copyedited and formatted. The final version may differ from this version.

Tables

Table 1: Demographics for hepatocyte donors used in the HepatoPac model

Demographics	Donor 1	Donor 2[a]	Donor 3[b]	Donor 4[c]	Donor 5[d]
Gender	Female	Male	Female	Female	Male
Age	19	56	54	61	31
Race/Ethnicity	Caucasian	African American	Caucasian	Not provided	Caucasian
Cause of Death	Intracerebral Bleed Secondary to ICH/Stroke	Cerebrovascular accident (CVA)	Anoxia secondary to CVA	Not provided	Anoxia, 2nd to heroin overdose
Medical History	Lupus	Diabetes, hypertension, kidney disease, insulin	Diabetes and hypertension, 3 years, med compliant	Not provided	Asthma: Allergy induced
Social History	No alcohol, tobacco or drug use	No alcohol, tobacco or drug use	Non-smoker, social drinker	Not provided	ETOH, Tobacco, Marijuana, Oxycontin, Heroin

[a] This donor was determined through genotyping analysis to be CYP3A5 *1*3
[b] This donor was determined through genotyping analysis to be CYP3A5 *3*3
[c] This donor was designated as RTM by the manufacturer
[d] This donor was designated as Donor 1307 by the manufacturer and was determined through genotyping analysis to be CYP3A5 *3*3

DMD Fast Forward. Published on June 15, 2015 as DOI: 10.1124/dmd.115.065326
This article has not been copyedited and formatted. The final version may differ from this version.

Table 2: Details of the smartpool Accell CYP3A4 siRNA

	Catalog #	Amount (nmol)	Sequence details	Mol wt (g/mol)
Non-targeting	D-001910-01-20	20	NA	NA
CYP3A4	E-008169-00-0010	10	CCGUUGUUCUAAAGGUUGA	13517.5
			UCCCAAUUCUUGAAGUAUU	13528.2
			GGAGUAUUCUAUAAGUUUU	13517.1
			GUUUUGAUUUAAUGUUUUC	13506.8

DMD Fast Forward. Published on June 15, 2015 as DOI: 10.1124/dmd.115.065326
This article has not been copyedited and formatted. The final version may differ from this version.

Table 3: Resulting $t_{1/2}$ (h) and k_{deg}^{-hr} values from individual donors and the combined average and standard deviations using the mono-exponential decay equation

Parameter	Donor 1	Donor 2	Donor 3	Donor 4	Donor 5
$t_{1/2}$ (h)	32.2	38.9	32.3	21.9	25.2
CYP3A k_{deg}^{-hr}	0.0215	0.0178	0.0215	0.0316	0.0275
R^2	0.900	0.954	0.889	0.949	0.975
CYP3A average $t_{1/2}$ (h) (all donors)		28.9			
CYP3A $t_{1/2}$ (h) Standard deviation		6.7			
CYP3A average k_{deg}^{-hr}		0.0240 ± 0.005			
CYP3A4 average (excluding donor 2)		27.2			
CYP3A4 Standard deviation		5.2			
CYP3A4 k_{deg}^{-hr}		0.0255 ± 0.005			

DMD Fast Forward. Published on June 15, 2015 as DOI: 10.1124/dmd.115.065326
This article has not been copyedited and formatted. The final version may differ from this version.

Table 4: Results of analyzing CYP3A enzyme recovery data upon removal of 10,000 or 1,000 pg/mL of IL6 with Equation 6

K_{deg} (1/h)	SE (CV %)	95% CI	R^2	AIC	Comments
0.0131	14.85%	[0.008115, 0.01814]	0.969	-17.1	Removal 1,000 pg/mL of IL6
0.0111	18.75%	[0.005735, 0.01641]	0.951	-13.6	Removal 10,000 pg/mL of IL6

DMD Fast Forward. Published on June 15, 2015 as DOI: 10.1124/dmd.115.065326
This article has not been copyedited and formatted. The final version may differ from this version.

Table 5: Results of analyzing CYP3A enzyme recovery data upon removal of 10,000 or 1,000 pg/mL of IL6 with Equation 11 and 12

Parameter	Estimate (h^{-1})	SE (CV %)	95% CI	R^2	AIC	Removal of treatment (IL6)
k_{deg} (assuming $k_{deg,RNA}$=0.0282 h^{-1})	0.0335	7.76%	[0.0268, 0.00402]	0.996	-31.5	1,000 pg/mL
	0.0231	11.7%	[0.0161, 0.0300]	0.992	-24.2	10,000 pg/mL
$k_{deg,RNA}$ (assuming k_{deg} =0.0316 h^{-1})	0.0296	6.50%	[0.0247, 0.0346]	0.996	-31.5	1,000 pg/mL
	0.0213	10.7%	[0.0154, 0.0271]	0.992	-24.1	10,000 pg/mL

DMD Fast Forward. Published on June 15, 2015 as DOI: 10.1124/dmd.115.065326
This article has not been copyedited and formatted. The final version may differ from this version.

A

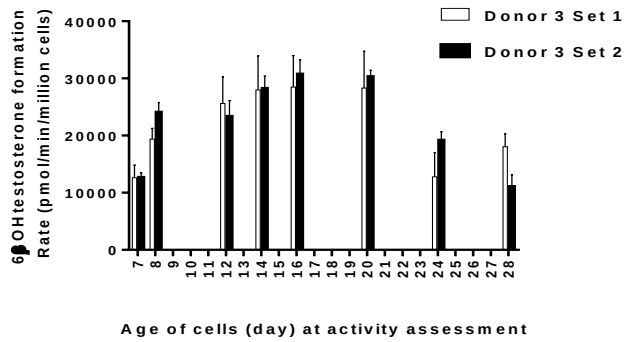

B

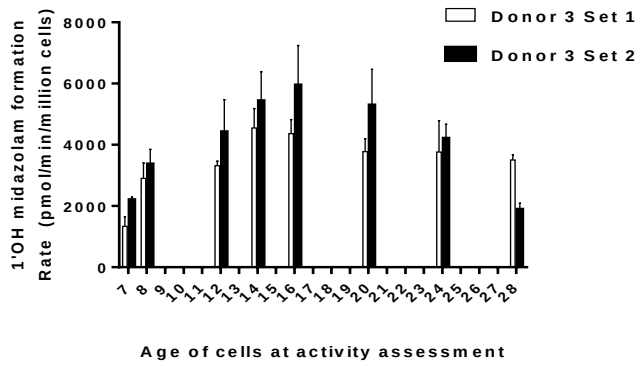

C

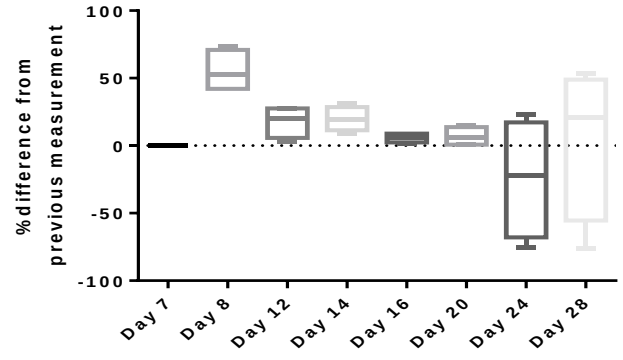

Figure 1

DMD Fast Forward. Published on June 15, 2015 as DOI: 10.1124/dmd.115.065326
This article has not been copyedited and formatted. The final version may differ from this version.

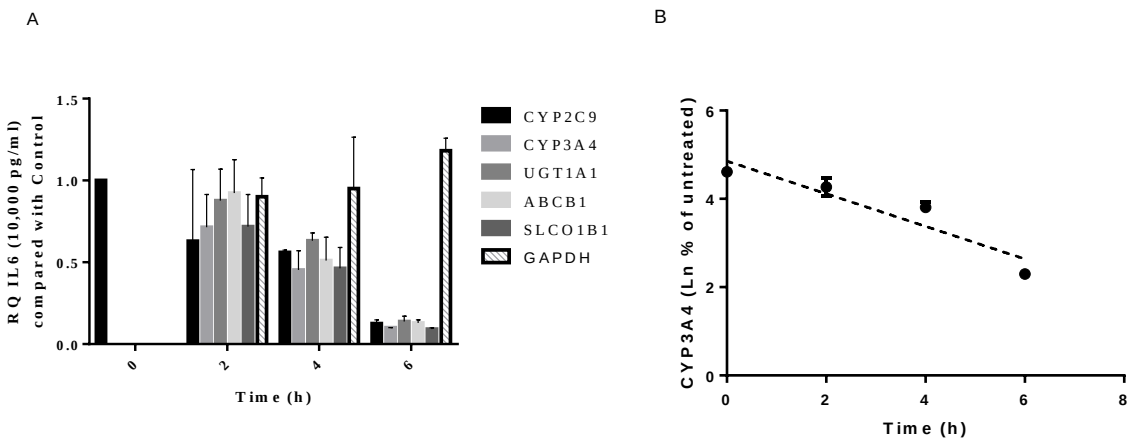

Figure 2

DMD Fast Forward. Published on June 15, 2015 as DOI: 10.1124/dmd.115.065326
This article has not been copyedited and formatted. The final version may differ from this version.

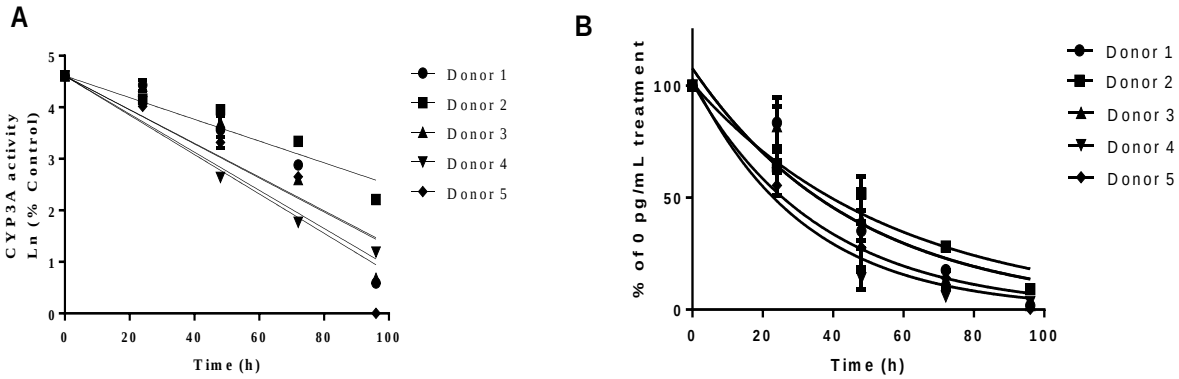

Figure 3

DMD Fast Forward. Published on June 15, 2015 as DOI: 10.1124/dmd.115.065326
This article has not been copyedited and formatted. The final version may differ from this version.

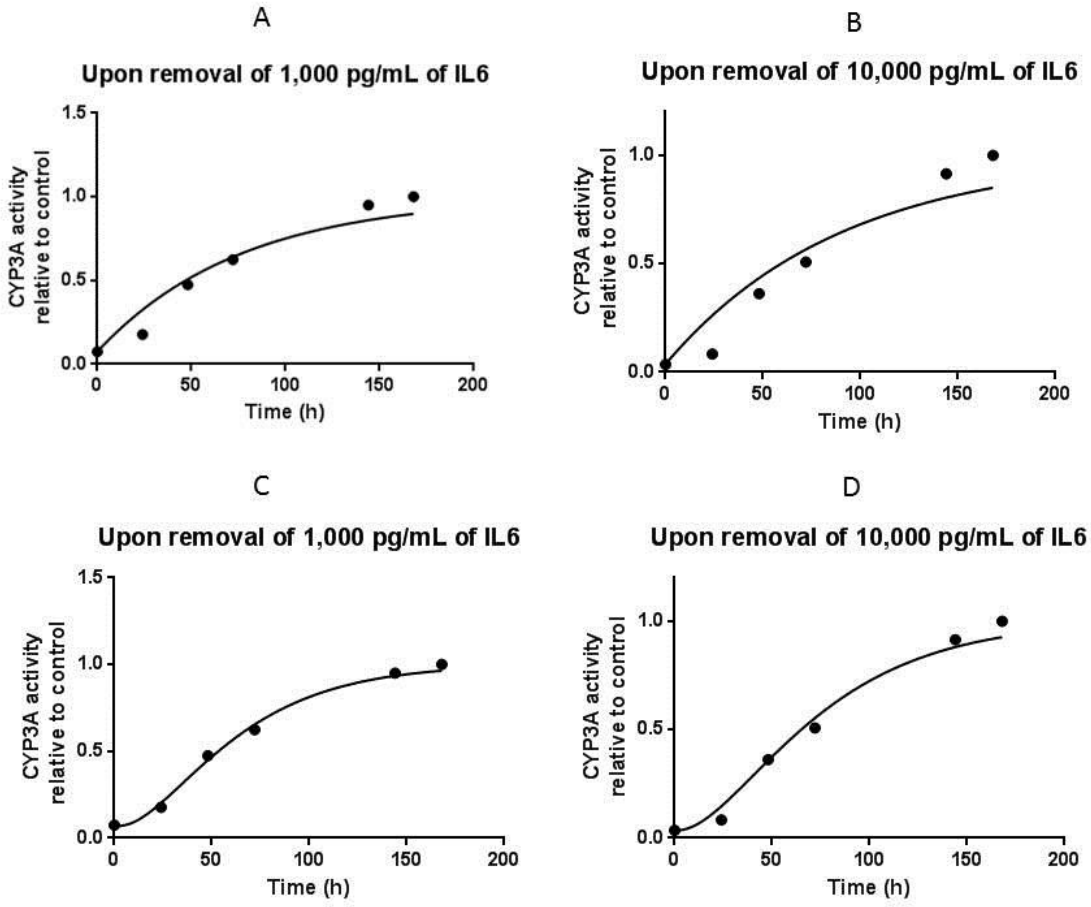

Figure 4

DMD Fast Forward. Published on June 15, 2015 as DOI: 10.1124/dmd.115.065326
This article has not been copyedited and formatted. The final version may differ from this version.

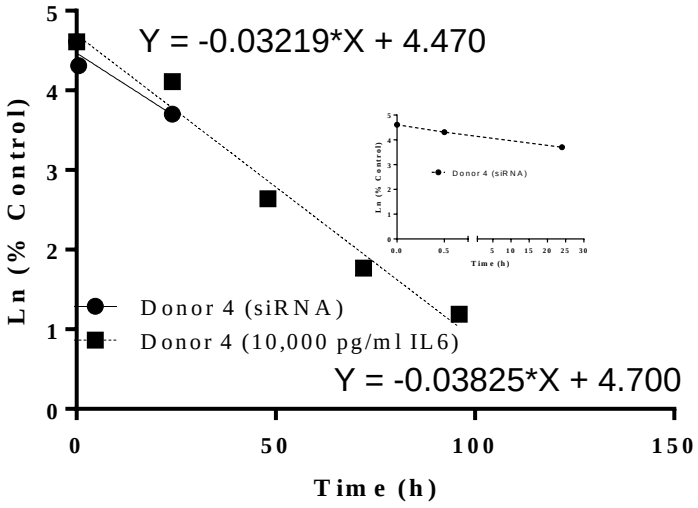

Figure 5